Measuring the temperature of high-luminous exitance surfaces with infrared thermography in LED applications

Indika U. Perera* and Nadarajah Narendran
Lighting Research Center, Rensselaer Polytechnic Institute, 21 Union St., Troy, NY 12180

ABSTRACT

Recently, light-emitting diode (LED) lighting systems have become popular due to their increased system performance. LED lighting system performance is affected by heat; therefore, it is important to know the temperature of a target surface or bulk medium in the LED system. In-situ temperature measurements of a surface or bulk medium using intrusive methods cause measurement errors. Typically, thermocouples are used in these applications to measure the temperatures of the various components in an LED system. This practice leads to significant errors, specifically when measuring surfaces with high-luminous exitance.

In the experimental study presented in this paper, an infrared camera was used as an alternative to temperature probes in measuring LED surfaces with high-luminous exitance. Infrared thermography is a promising method because it does not respond to the visible radiation spectrum in the range of 0.38 to 0.78 micrometers. Usually, infrared thermography equipment is designed to operate either in the 3 to 5 micrometer or the 7 to 14 micrometer wavelength bands. To characterize the LED primary lens, the surface emissivity of the LED phosphor surface, the temperature dependence of the surface emissivity, the temperature of the target surface compared to the surrounding temperature, the field of view of the target, and the aim angle to the target surface need to be investigated, because these factors could contribute towards experimental errors. In this study, the effects of the above-stated parameters on the accuracy of the measured surface temperature were analyzed and reported.

Keywords: light-emitting diodes, LED lighting system, testing, lens temperature, surface temperature, IR thermography, measurement error, surface emissivity

1. INTRODUCTION

Light-emitting diode (LED) technology has improved significantly over the past decade. The technology has now reached a level where LED chips emit high radiant power, in the order of watts per chip. To create "white" light for illumination applications, the emission of these LED chips are combined with phosphor-encased optical encapsulant layers.[1] Past studies report increases in LED package lumen degradation due to both chip and encapsulant degradation caused by high temperature.[2],[3] In order to quantify LED lens degradation and improve LED performance, as well as for safety-related aspects, it is necessary to measure the lens temperature accurately during operation. With increased demand for larger lumen packages with smaller LED package footprint area, the lumen output and therefore luminous flux densities of these lenses increase. The luminous flux exiting or leaving a surface is termed as luminous exitance.[4]

In measuring the bulk medium or surface temperature of these LED lenses, either contact (intrusive) or non-contact type measurement methods can be employed. Intrusive-type measurements are commonly conducted with thermocouples. These thermocouple measurements are reported to have significant errors caused by the optical radiation emitted through the lens surface being measured.[5],[6] In addition, measurement errors can be caused by the geometrical configuration, attachment method, and heat transfer interactions of intrusive-type temperature measurements.[7] Infrared temperature measurement systems are non-contact type measurement methods that lack some of the stated sources of error such as attachment method and heat transfer interaction present in contact-type methods. Infrared temperature measurement systems are generally designed to be sensitive between 3–5 μm and 7–14 μm wavelength bands.[8] The optical emission of an LED system used for illumination is in the range of ~0.4–0.8 μm where the infrared temperature measurement systems are insensitive.

*Corresponding author: pereru2@rpi.edu; +1 (518) 687-7100; www.lrc.rpi.edu/programs/solidstate

Fifteenth International Conference on Solid State Lighting and LED-based Illumination Systems,
edited by Matthew H. Kane, Nikolaus Dietz, Ian T. Ferguson, Proc. of SPIE Vol. 9954,
99540K · © 2016 SPIE · CCC code: 0277-786X/16/$18 · doi: 10.1117/12.2240650

Infrared temperature measurements have been used in the electronics and LED industries to measure surface temperatures as an alternative to contact-type temperature measurements.[9],[10] The calibration of the infrared temperature measurement system is very important to obtaining an accurate, repeatable measurement.[8]

In order to estimate the target surface temperature, the emissivity of the target surface becomes a prerequisite for accurate estimation. Additionally, the range of temperatures during operation that might cause changes to the target surface emissivity and geometric configurations, such as infrared temperature measurement system aiming angle, distance, background temperature and surface emissivity of the target, can also affect the estimated temperature. This study investigated the effect of these parameters on the LED lens surface temperature.

2. METHODOLOGY

This study is mainly concerned with investigating and quantifying measurement errors associated with the systematic error with using infrared temperature measurement systems. Calibration of the infrared temperature measurement system was not investigated nor discussed, and it is assumed that the measurement system is in calibration.

A number of methods are available in literature to characterize an unknown target surface.[8] Due to the practical difficulties of these methods, an alternative two-stage method was developed using a flat-black paint coat as the reference.

In the first stage, the selected reference paint coated on a target surface was characterized. Then the characterized paint was coated on one-half of the LED lens surface. The different material surfaces were then characterized based on temperature comparison with the characterized paint-coated surface. Then the surface temperature during operation of the LED module was estimated using the infrared imaging camera based on the experimentally determined surface characteristics.

3. EXPERIMENT

A single-band wavelength infrared imaging camera module with a focal plane array detector (FPA) having a sensitive spectral range from 7.5–14 μm (Jenoptik IR-TCM 384 with a 384×244 pixel resolution of bolometric FPA detector) was used for the study. Figure 1 illustrates the experimental setup used for the characterization of the black paint (Rust-Oleum V2178838 high-temperature spray paint) coated surface. The experimental setup had the ability to independently rotate the black-coated surface in the two perpendicular axes (indicated by the black arrows) on the horizontal plane with the pivot axis remaining horizontal.

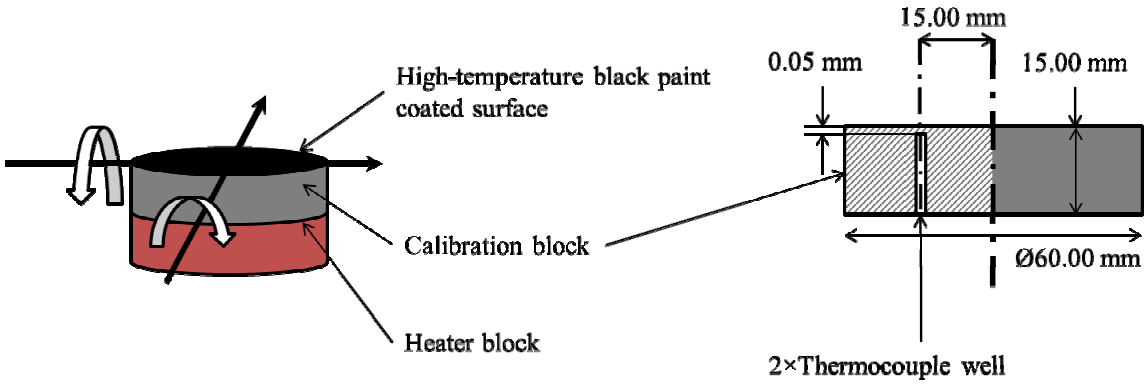

Figure 1. Schematic of the high-temperature black paint characterization experimental setup.

3.1 Characterization of the applied paint coating

The infrared imaging camera was aimed normal to the crossing-point of the pivot axes on the black paint-coated surface and the entire setup was placed ~50 mm from the optics of the thermal imager. This was to ensure the entire field of view (FOV) of the thermal imager was covered by the black paint-coated surface of the calibration block, as indicated in Figure 2. To facilitate the heating of the black paint-coated surface to different temperature values, the calibration block was mounted on a heater block. Two calibrated, J-type 30 AWG thermocouples were embedded in machined blind holes

in the aluminum calibration block. The cross section on the right of Figure 1 indicates the dimensions of the calibration block and the blind holes for the thermocouples (thermocouple wells).

An Omega TC-08 8-channel USB thermocouple data acquisition module was used to acquire the temperature from the thermocouples. The thermocouples and the data acquisition system were checked for calibration using a Fluke 714B thermocouple calibrator.

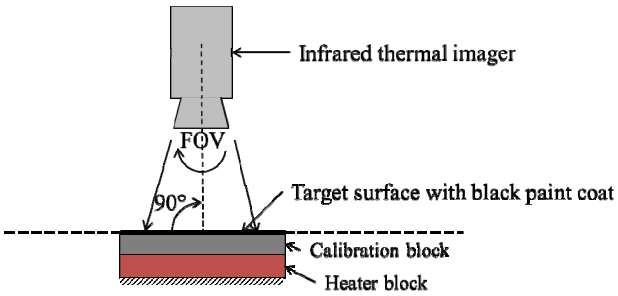

Figure 2. Schematic diagram of the infrared thermal imager and experimental setup.

The heater block was heated to a number of predefined temperature values and once steady-state was achieved with respect to the embedded thermocouple measurements, the infrared thermal imager was used to estimate the surface temperature. Figure 3 illustrates the infrared imaging camera-estimated temperature vs. the thermocouple-measured temperature. The line running diagonally across the chart is provided as a visual guide to illustrate the ideal temperature that the infrared thermal imager should have estimated at a given thermocouple-measured temperature. This shows the default surface emissivity of ε=1.00 (ideal blackbody) overestimated the temperature at temperatures ≤40°C and underestimated the surface temperature at temperatures ≥80°C. The deviation from the thermocouple-measured temperature was greater than ±1.5 K between 0 and 100°C and ±2% of the measured temperature (based on thermal imager measurement accuracy).[11] Figure 3 shows that the paint coating's surface emissivity decreases with increasing temperature.

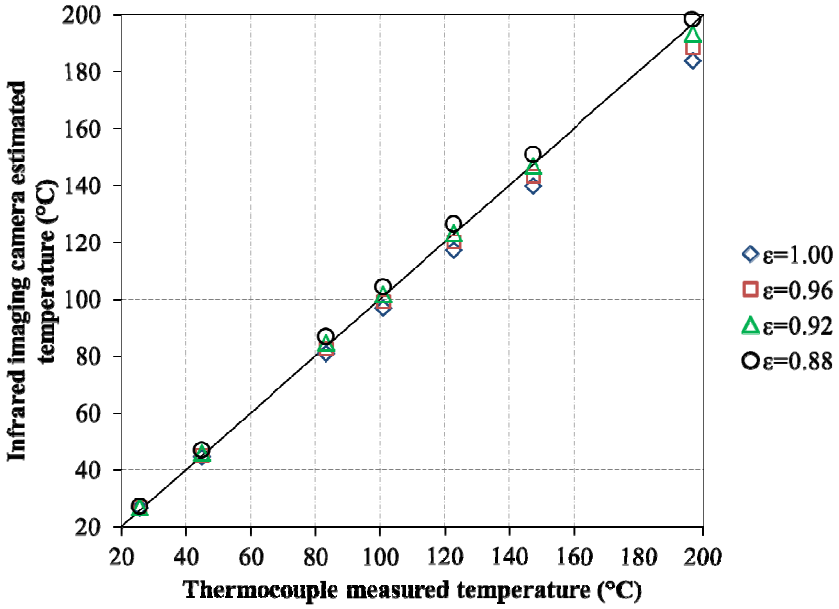

Figure 3. Characterization of the surface emissivity of the black paint-coated surface.

Table 1 shows the effective surface emissivity calculated to have the minimum error between the thermocouple-measured temperature and the infrared thermal imager-estimated temperature. These estimated effective surface emissivity values were used in the subsequent estimation of surface temperature.

Table 1. Effective surface emissivity of black paint-coated surface.

Temperature range (°C)	Effective surface emissivity
≤80	0.96
>80–≤160	0.92
>160–200	0.90

The calibration block was rotated both in the positive and negative direction on one axis (according to the right-hand rule) at a time, as illustrated in Figure 1, while maintaining the surface temperature constant. The surface temperature was varied to three distinct temperature values while measuring the temperature using the embedded thermocouples. Figure 4 indicates the variation of the infrared thermal imager-estimated temperature after adjusting for the temperature-dependent emissivity change with the thermocouple-measured temperature. The infrared thermal imager-estimated temperature represents the mean temperature of four measurements except for the 0° temperature measurement. For aiming angles less than 30° from the surface normal of the target surface and thermal imager optical axis, the deviation from the thermocouple-measured temperature was less than the measurement accuracy of the device at the tested temperatures. A greater deviation more than the measurement accuracy of the thermal imager was observed when the rotation angle exceeded 30° for surface temperatures above ~50°C.

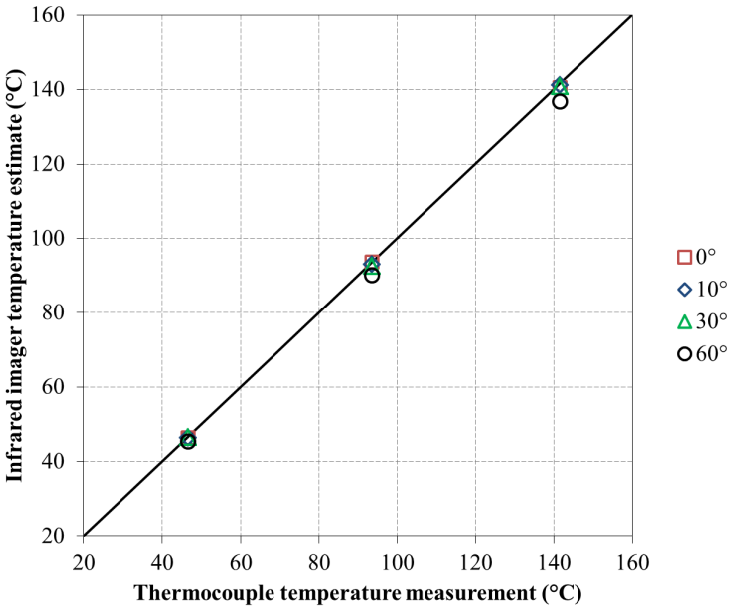

Figure 4. Angular dependence of infrared thermal imager temperature estimate.

To assess the effect of FOV and target background emissivity, a similar experiment was conducted with the normal of the black paint-coated surface on axis with the infrared thermal imager, as indicated in Figure 5. The distance from the thermal imager optics to the background plate was varied to change the FOV of the black paint-coated surface. In addition, the surface emissivity of the background plate was also changed by interchanging the plates with the same high-temperature black paint ($\varepsilon>0.9$) and with no surface coating ($\varepsilon<0.2$). The background surface temperature was maintained at 25±2°C.

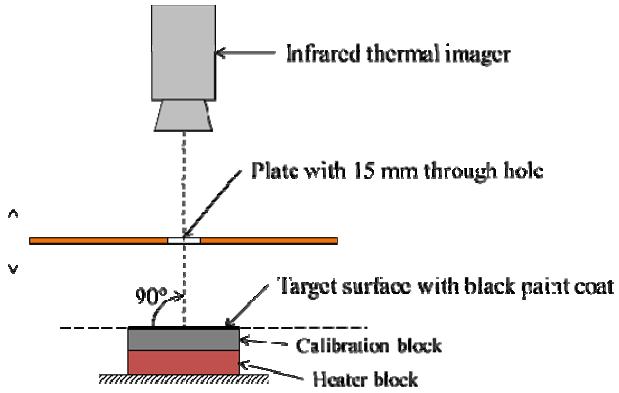

Figure 5. Configuration of the experimental setup for FOV and background effects.

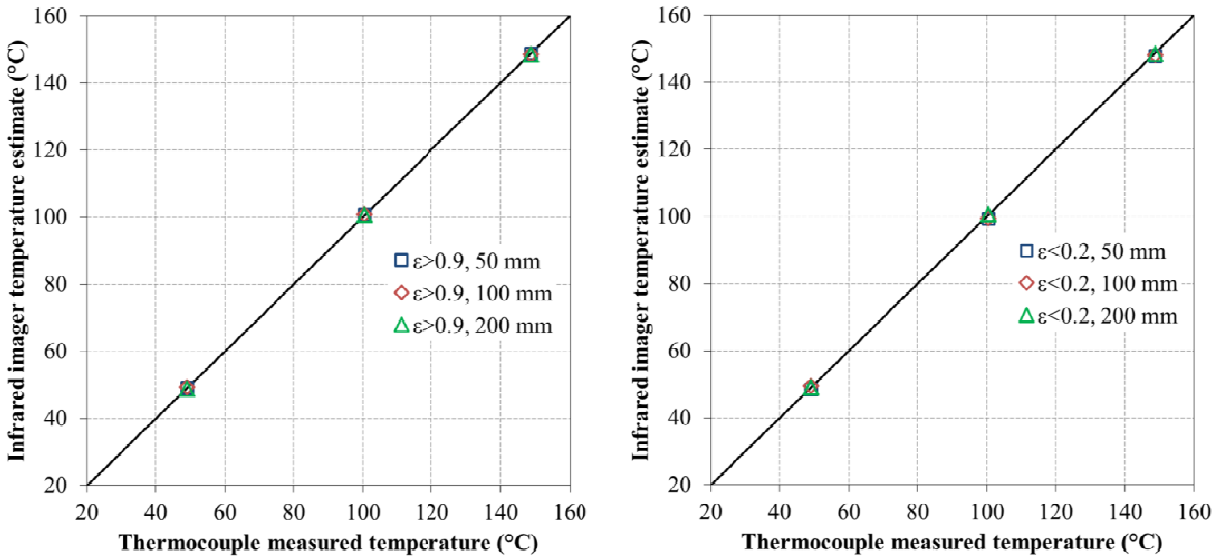

Figure 6. FOV and background emissivity effect on infrared thermal imager-estimated temperature: background surface emissivity ε>0.9 (left) and background surface emissivity ε<0.2 (right).

Figure 6 shows there was no significant effect on the infrared thermal imager-estimated temperature when compared with the thermocouple-measured temperature. The 50 mm distance corresponded to a FOV 300 mrad, and the 200 mm distance corresponded to a FOV 75 mrad.

In order to assess the effect of background temperature on the infrared thermal imager-estimated temperature, the same experimental setup was used with the added feature of heating the plate with the through hole illustrated in Figure 5. Figure 7 shows the observed results from the experiment. The infrared imager-estimated temperatures were within the measurement accuracy of the device with the thermocouple-measured temperature values.

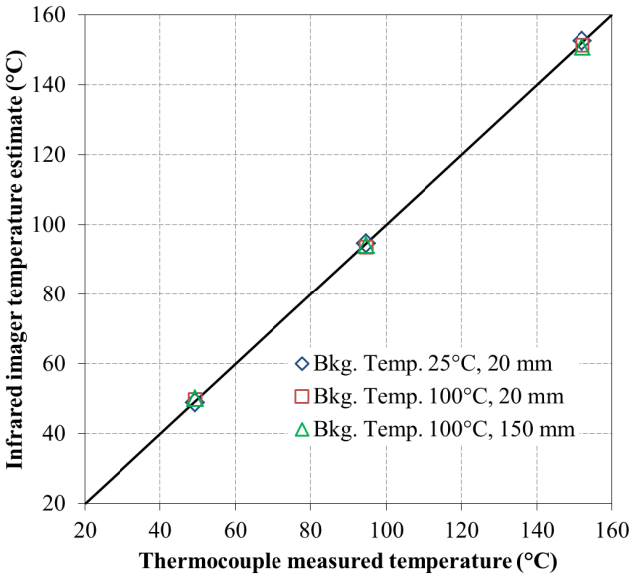

Figure 7. Background temperature effect on infrared thermal imager temperature estimate.

3.2 Characterizing LED module surface

These initial experiment results showed that the major systematic error stems from surface emissivity adjustments followed by angular-dependent errors at aiming angles larger than 30°. In order to estimate the LED lens exitance surface temperature, the LED module was coated with the characterized black paint on half the surface, as illustrated in Figure 8. Then the LED module was mounted on a heater block and the infrared thermal imager was used to assess the emissivity values for the different material surfaces in the LED module. At any steady-state temperature, the LED module components are approximately at the same temperature. Along the line of symmetry, the temperature on either side of the coated and uncoated halves is assumed identical. The surface emissivity of the black-coated side was adjusted to the predetermined value based on the paint characterization. Then the unknown material surface emissivity was adjusted until the two temperature values matched.

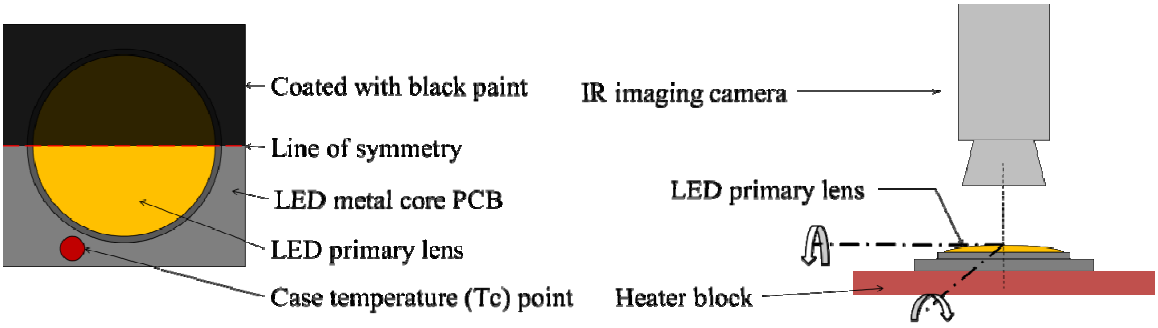

Figure 8. Schematic of the LED module and orientation for the experiment with the infrared thermal imager.

Figure 9 shows the temperature matching of the black paint-coated surface and the silicone surface of the LED primary lens. It also shows the angular variation of the estimated temperature. The estimated temperature on the same location close to the geometric center of the LED module indicated a larger spreading of the estimated temperature as the LED module was rotated along the horizontal axes with increasing temperature. This was due to the geometry of the LED lens surface. The flat areas of the LED module used to assess the emissivity of the solder mask did not show a similar trend with increase in temperature.

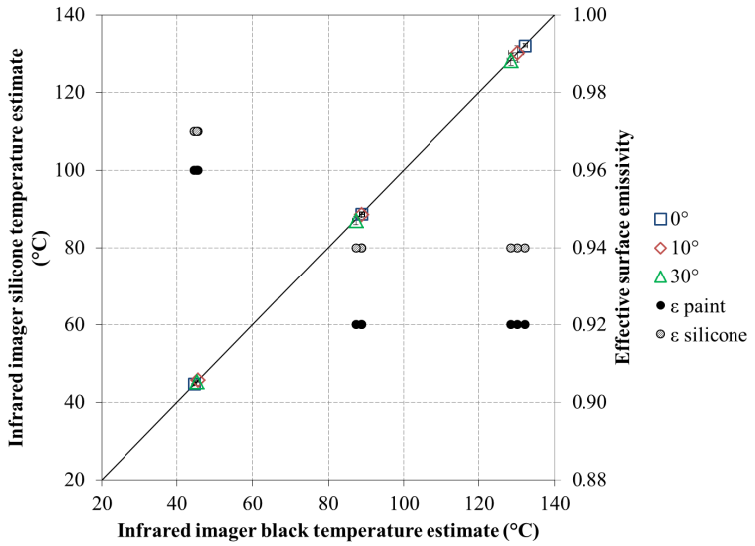

Figure 9. Evaluation of LED primary lens emissivity by matching temperature.

3.3 Estimating high-luminous exitance surface temperature

Two identical samples of the same LED module that was used in the characterization process were selected, and one module was coated with the same black paint while the other was uncoated. The black coating was sufficient in eliminating luminous flux (optical radiation) from being emitted from the primary lens surface. Both LED modules were mounted on heat sinks and operated in constant current mode. The infrared thermal imager and J-type 36 AWG Perfluoroalkoxy (PFA) insulated thermocouples (Omega SRTC-TT-J-36-36) were used alternately to measure the LED lens temperature at the geometric center of the lens exitance surface at the same drive current conditions. The case temperature of the LED module was also measured using both the infrared thermal imager and the same type of J-type thermocouples. To attach the thermocouple to the LED lens exitance surface, an optical silicone elastomer (NuSil CV-2500 Silicone, Two Part Adhesive and Sealant) was used and was removed after each measurement with the infrared thermal imager. A two-part permanent adhesive (Arctic Alumina Thermal Adhesive) was used to attach the thermocouple at the case temperature location.

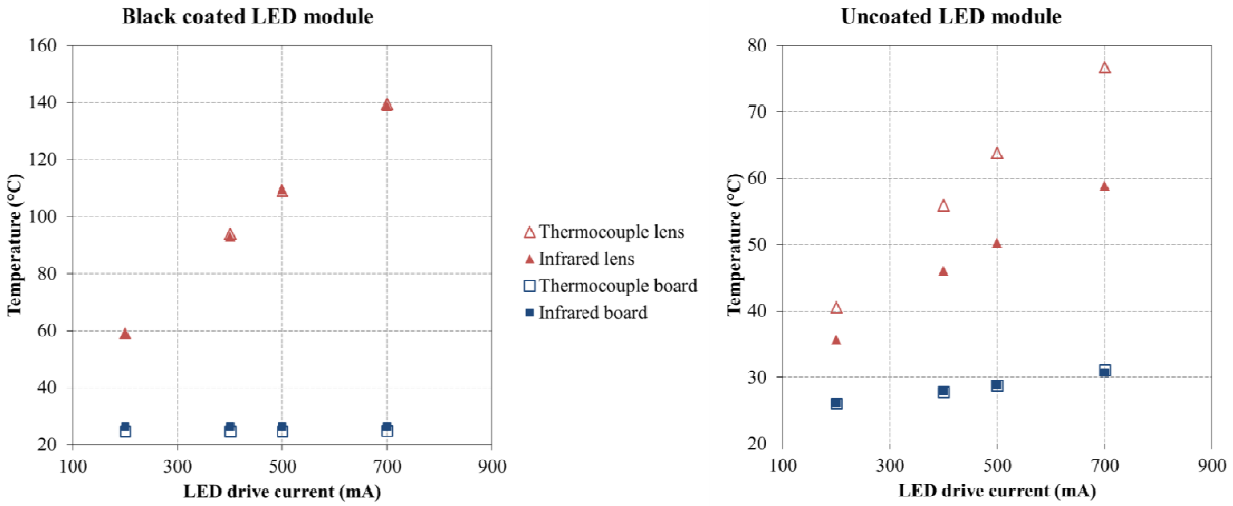

Figure 10. Infrared thermal imager and thermocouple temperature measurements of the energized LED module.

Figure 10 shows the infrared imager- and thermocouple-measured temperatures at the geometric center of the lens and the case temperature location of the black paint-coated (no radiant flux-emitting LED module) and the uncoated LED

modules. The thermal imager temperature estimates after adjusting for the temperature-dependent emissivity of the black paint coating matched the thermocouple measurement both at the geometric center of the lens and at the LED module case temperature location.

The uncoated LED module case temperature measurements from the thermal imager and the thermocouple also matched after adjusting for the solder mask surface emissivity, which was found during the characterization stage. This validated the characterization process used for the thermal imager temperature estimation. Then the luminous exitance surface geometric center was measured with the infrared imager and adjusted for the surface emissivity of the silicone, which was assessed during the characterization stage. Figure 10 also indicates the thermocouple measurement at the geometric center overestimated the surface temperature due to the absorption of the optical radiation.[5],[6]

A prototype LED light engine was designed with an LED array consisting of 21 Cree XLamp XP-E2 royal blue LED packages (XPEBRY-L1-0000-00P01) arranged in an array to provide a uniform irradiance on the silicone layer and the silicone layer heat sink, as illustrated in Figure 11. The LEDs were operated at a 700 mA constant current (Agilent E3634A dc power supply×2). A silicone elastomer (NuSil CV-2500 Silicone, Two Part Adhesive and Sealant) was used to create a silicone layer (diameter of 4 mm and 1 mm thick) and was embedded in an aluminum heat sink 60×60×1 mm^3. The aluminum heat sink was attached to a heating element to control the temperature of the silicone layer. A J-type 36 AWG Perfluoroalkoxy (PFA) insulated thermocouple was used to measure the temperature of the silicone layer heat sink near the silicone layer on the side facing away from the LED irradiance. The diameter of the phosphor layer was selected to maintain a uniform temperature distribution on top of the silicone layer, which is at the same heat sink temperature based on past studies.[12]

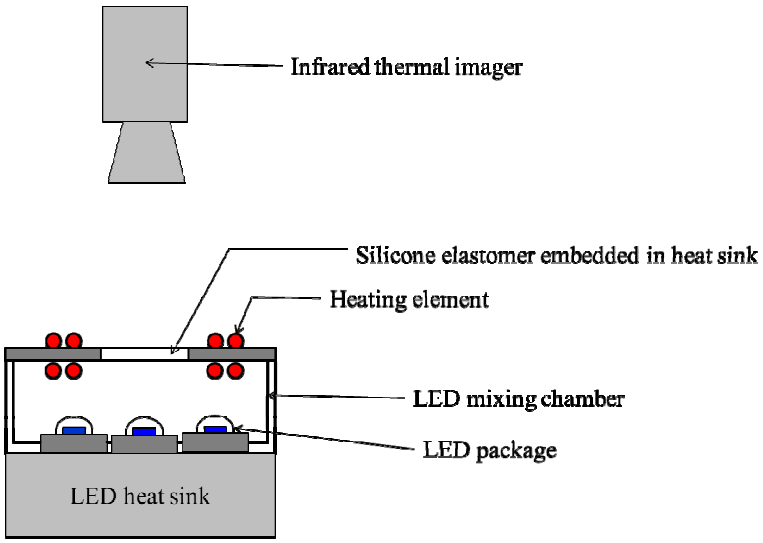

Figure 11. Schematic of the LED light engine with heated silicone layer experiment setup.

Figure 12 shows the silicone layer temperature estimated using the infrared thermal imager after a similar characterization of the surface emissivity as described in the previous sections. This temperature is compared with the thermocouple measurement of the heat sink temperature. The error bars represent the minimum to maximum temperature range of three measurements. The estimated temperature from the infrared thermal imager was within the higher of 1.5 K or 2% of the measured temperature at all conditions.

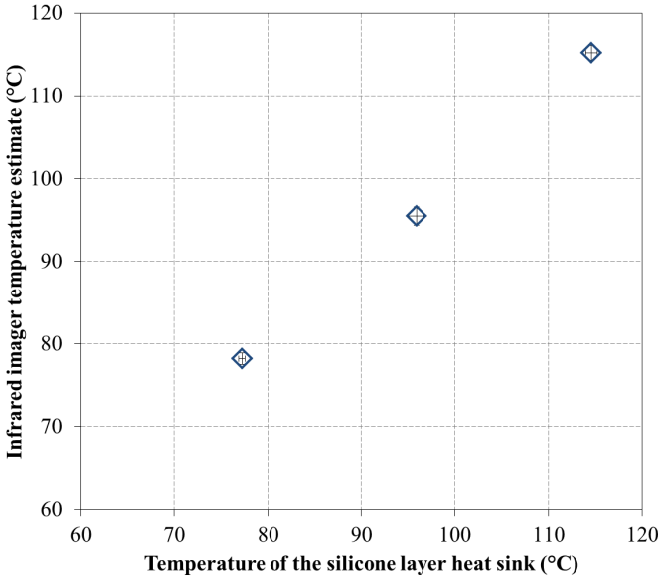

Figure 12. Infrared imager temperature estimate of the silicone layer with luminous exitance surface.

4. CONCLUSIONS

The infrared thermal imager was able to predict the surface temperature of the luminous exitance surfaces to within the measurement accuracy after the surface emissivity adjustments and maintaining the aiming angle below 30°. These factors were the main sources of systematic error in the estimated temperatures from the infrared thermal imager.

ACKNOWLEDGMENTS

The authors would like to acknowledge the Alliance for Solid-State Illumination Systems and Technologies (ASSIST # H11014), the Federal Aviation Administration (FAA Research Grant Number 13-G-009), Rensselaer Polytechnic Institute and the Lighting Research Center (IRA) for financial assistance during this research project.

The authors would like to acknowledge the efforts of Jennifer Taylor of the Lighting Research Center for her invaluable assistance in preparation of this manuscript and the staff at the Lighting Research Center.

REFERENCES

[1] Mueller-Mach, R. and Mueller, G.O., "White-light-emitting diodes for illumination," *Proc. SPIE* 3938, 30–41 (2000); doi: 10.1117/12.382840.

[2] Barton, D.L. *et al*., "Life tests and failure mechanisms of GaN/AlGaN/InGaN light emitting diodes," *Proc. SPIE* 3279, 17–27 (1998); doi: 10.1117/12.304426.

[3] Tamura, T. *et al*., "Illumination characteristics of lighting array using 10 candela-class white LEDs under AC 100 V operation," *J. Luminescence* 87-89, 1180–1182 (2000); doi: 10.1016/S0022-2313(99)00588-8.

[4] Murdoch, J.R., "Introducing Light and Seeing," in *Illumination Engineering: from Edison's Lamp to the LED*, 2nd ed., ch. 1, sec. 7, pp. 20-30, Vision Communications, New York (2003).

[5] Perera, I.U. *et al*., "Accurate measurement of LED lens surface temperature," *Proc. SPIE* 8835, 883506-1-6 (2013); doi: 10.1117/12.2023091.

[6] Fu, X. and Luo, X., "Can thermocouple measure surface temperature of light emitting diode module accurately?" *Int. J. Heat and Mass Transfer* 65, 199-202 (2013); doi: 10.1016/j.ijheatmasstransfer.2013.05.072.

[7] Figliola, R.S. and Beasley, D.E., [Theory and Design for Mechanical Measurements, 5th ed.], John Wiley and Sons Inc., Hoboken, NJ, 309–367 (2011).

[8] Kaplan H., [Practical Applications of Infrared Thermal Sensing and Imaging Equipment, 3rd ed.], SPIE-International Society for Optics and Photonics, Bellingham, WA (2007).

[9] Garg, J. *et al.*, "Micro fluidic jets for thermal management of electronics," *Proc. ASME 2004 Heat Transfer/Fluid Engineering Summer Conference 4*, 647–654 (2004); doi: 10.1115/HT-FED2004-56782.

[10] Arik, M. and Stanton, W., "Effect of chip and bonding defects on the junction temperatures of high-brightness light-emitting diodes," *Optical Engineering* 44(11), 111305-1-8 (2005); doi: 10.1117/1.2130127.

[11] JENOPTIK Laser, Optik, Systeme GmbH, "*JENOPTIK IR-TCM 384 & 640 Manual,"* Revision 003 (2009).

[12] Perera, I.U., "Thermal management of remote phosphor layer in a light-emitting diode system," M.S. thesis, Dept. Lght., Rensselaer Polytechnic Institute, Troy, NY (2013).